Journal of Molecular Structure 1115 (2016) 1–7

Contents lists available at ScienceDirect

Journal of Molecular Structure

journal homepage: http://www.elsevier.com/locate/molstruc

Photoelectron spectra and electronic structure of nitrogen analogues of boron β-diketonates

Sergey A. Tikhonov [a, *], Vitaliy I. Vovna [a], Aleksandr V. Borisenko [b]

[a] Far Eastern Federal University, 8 Sukhanova St., Vladivostok, 690950, Russia
[b] Vladivostok Branch of Russian Customs Academy, 16v Strelkovaya St., Vladivostok, 690034, Russia

ARTICLE INFO

Article history:
Received 2 December 2015
Received in revised form
22 February 2016
Accepted 22 February 2016
Available online 24 February 2016

Keywords:
Electronic structure
Chelate complexes
Boron β-diketonates
Nitrogen analogues
Photoelectron spectroscopy
Density functional theory

ABSTRACT

The electronic structure of the valence levels of seven nitrogen-containing boron complexes was investigated using methods of ultraviolet photoelectron spectroscopy and density functional theory. The ionization energies of π- and σ-levels were obtained from photoelectron spectra. The electronic structure of nitrogen-containing compounds was compared with the electronic structure of β-diketonates. It was shown the influence of various substituents on carbon and nitrogen atoms of six-membered ring on the electronic structure of complexes. The changes in the electronic structure after the substitution of atoms in condensed cycles have been identified.

In order to compare the experimental vertical ionization energies IE_i with Kohn–Sham orbital energies ε_i we used the analogue of Koopmans theorem and average amendment to the orbital energy of the electrons ($\bar{\delta}_i$). For 26 electronic levels of seven studied complexes, the calculated values are in good accordance with experimental energy intervals between electron levels.

1. Introduction

Boron β-diketonates ($X_2B(O–C(R_1)–C(R_2)–C(R_3)–O)$ possess an intensive luminescence [1–5] and are used because of these properties as laser dyes [6], active components of solar thermal collectors [7] and materials for electrophotography [8]. Due to the high biological activity of boron β-diketonates [9,10], they are also used as antiviral drugs.

The determination of relationships between the functional characteristics of substances and their electronic structure opens up opportunities for the direct synthesis of new compounds with prescribed properties. The electronic structure of boron β-diketonates has been studied using absorption [11–15] and photoelectron [16,17] spectroscopy. Earlier, we published the results of our studies of the electronic structure of boron β-diketonates based on the ultraviolet photoelectron spectroscopy (UPS) of vapours [18–20], X-ray electron spectroscopy of molecular crystals [18,20] and density functional theory (DFT) [18–20] methods.

Nitrogen analogues of boron β-diketonates are also of scientific and practical interest [21–23], but their electronic structure, unlike that of boron β-diketonates, has not been previously investigated by the UPS method.

This paper presents the results of a study of the electronic structure of seven nitrogen analogues of boron β-diketonates using UPS method and DFT approach. The usage of DFT for description of ionization states is based on an analogy between the Dyson's quasiparticle equation and Kohn–Sham equation. The general Dyson's equation [24,25] can be transformed to the Dyson's one-electron equation for the theoretical description of ionization processes [26]. The Kohn–Sham orbitals may serve as a good approximation to Dysons' orbitals in the case of valence ionization [27]. That's why Kohn–Sham Eigen functions are interpreted as approximate relaxed Dyson's orbitals, and respective Kohn–Sham orbital energies ε_i are interpreted as approximate relaxed ionization potentials [28–30]. The validity of this statement was checked on the example of several atoms and simple molecules [31–33]. Also in Refs. [18–20] it is shown that DFT allows the calculation of the energies of ionized boron complex states with a high accuracy, thus providing a good theoretical basis for the unambiguous interpretation of photoelectron (PE) spectra and analysis of valent electron levels of compounds I–VII.

* Corresponding author.
E-mail address: allser@bk.ru (S.A. Tikhonov).

http://dx.doi.org/10.1016/j.molstruc.2016.02.075
0022-2860/

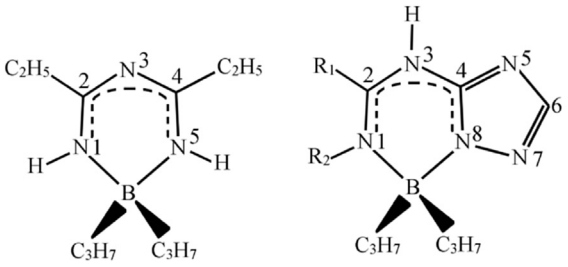

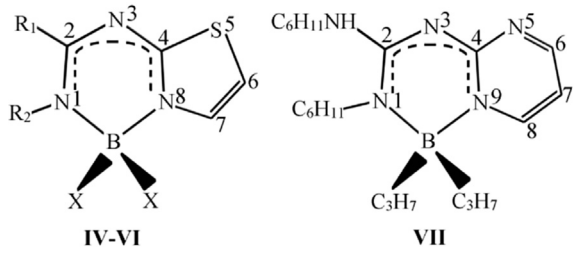

II. $R_1 = R_2 = H$
III. $R_1 = 4\text{-}C_6H_4CH_3$, $R_2 = H$
IV. $X = C_4H_9$, $R_1 = R_2 = H$
V. $X = C_4H_9$, $R_1 = 4\text{-}C_6H_4CH_3$, $R_2 = H$
VI. $X = C_3H_7$, $R_1 = C_6H_{11}NH$, $R_2 = C_6H_{11}$

The spectra were interpreted, with use of dependence of the amendment to orbital energy on the nature of the molecular orbital [18–20]. The calculated parameters of the electronic structure of complex I have been compared with the data on the isoelectronic β-diketonate complex Ia.

2. Experimental and calculation methods

Samples were synthesized in the N. D. Zelinsky Institute of Organic Chemistry (Moscow) using methods described in Refs. [34–37]. The PE spectra of vapours of compounds I–VII were obtained on an ES-3201, converted electronic spectrometer with a He I ($h\nu = 21.2$ eV) monochromatic radiation source. The error in the determination of band maximums was within 0.02 eV. The ionization cuvette temperature depended on the vapour sublimation temperature of a particular sample and varied in the range of 180 °C to 220 °C. All spectra have bands with good resolution in the range of 6.5–10 eV. There is band overlap due to the high density of states in the range of energies above 10 eV.

In our DFT quantum chemistry calculations, we applied the Firefly 7.1.G software program [38] using the 6-311G (d) basic set [39]. The calculation results depend on type of exchange-correlation functional. At the present time the hybrid functionals [40], double-hybrid functionals [41], Minnesota functionals [42] and range-separated functionals [43,44] are used for DFT calculations. The method of dispersion correction as an add-on to standard Kohn–Sham density functional theory [45] is also used. In this paper, we study boron chelates built from H, B, C, N, and O atoms. The hybrid three-parameter functional [15,46–48] are successfully used for DFT calculations of boron complexes. The goal of our research is the electronic structure in ground state and the interpretation of ultraviolet photoelectron spectra. In our review [49] it was shown that hybrid B3LYP5 functional [50–52] gives good results for investigation of electronic structure of boron complexes by UPS method. Because we used B3LYP5 functional in our previous researches [18–20], we used it in this paper too. This allows excluding the influence of functional type on the electronic effects of substitution.

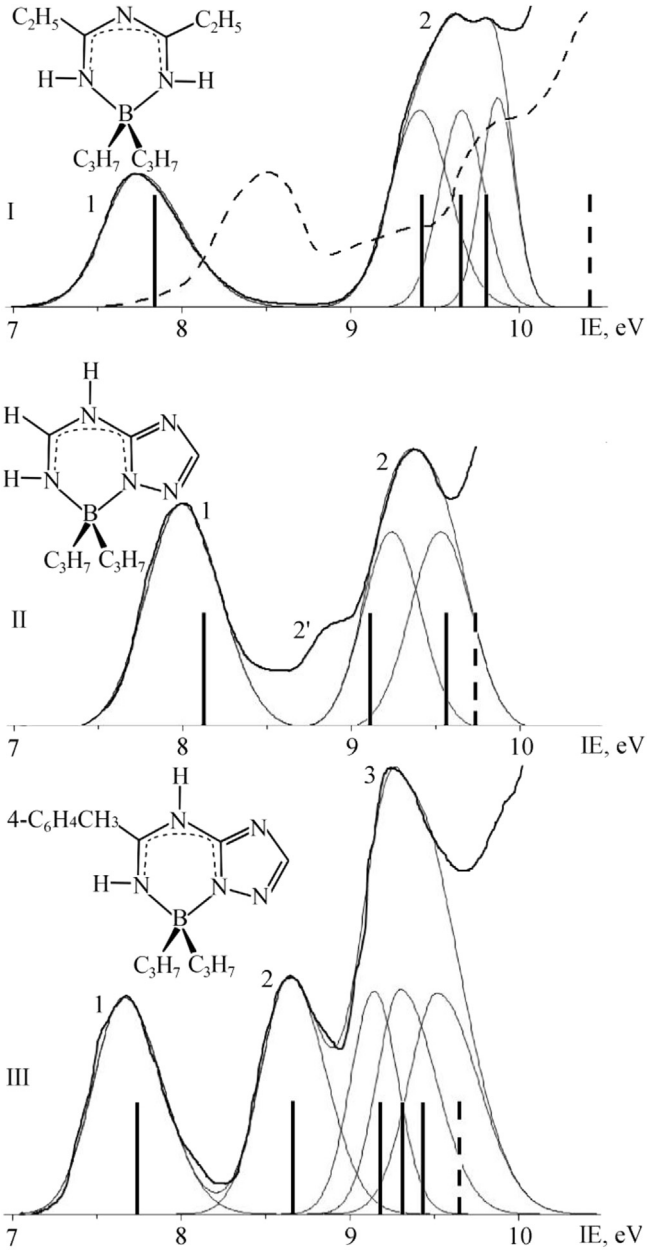

Fig. 1. Ultraviolet photoelectron spectra of the vapours of compounds I—III. The boron diethyl acetylacetonate spectrum [19] is indicated by a dotted line on the spectrum of compound I.

We calculated the Hessian matrix to check the correspondence between optimized structures and local minimum points on the potential energy surface. The absence of imaginary frequencies in the vibration spectrum indicated that minimum was reached on the surface of potential energy.

We used the analogue of Koopmans' theorem to compare the experimental values of vertical ionization energies (IE) with Kohn–Sham orbital energies ε_i:

$$IE_i = -\varepsilon_i + \delta_i$$

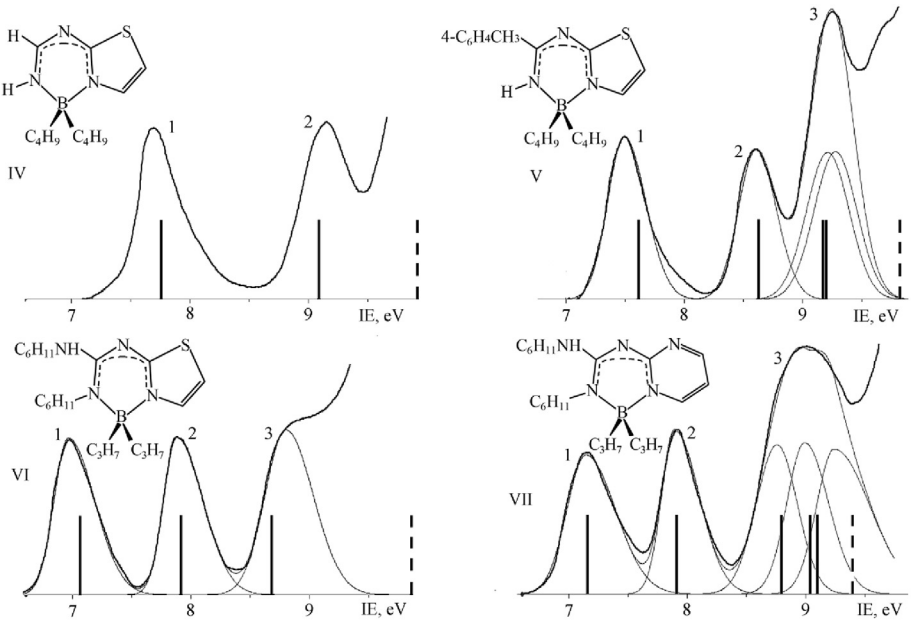

Fig. 2. Ultraviolet photoelectron spectra of the vapours of compounds IV—VII.

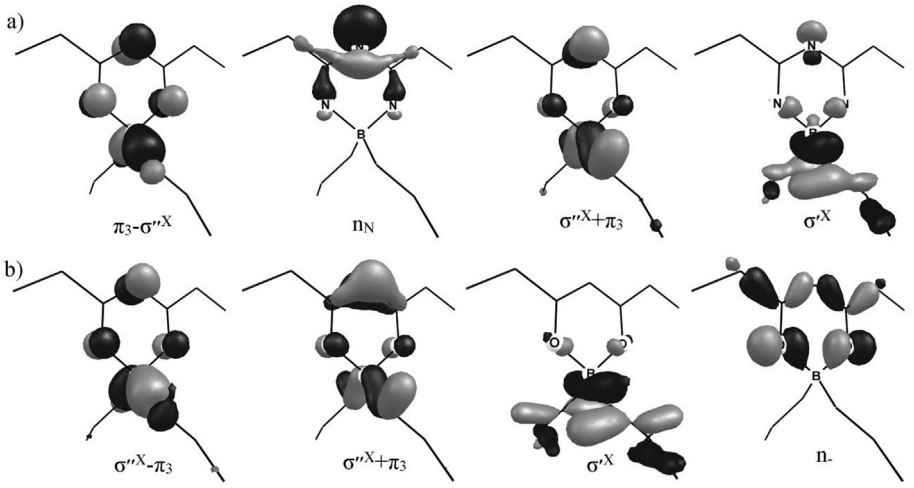

Fig. 3. Four upper occupied molecular orbitals of compounds I (a) and Ia (b).

where IE_i — ionization energy;ε_i — Kohn–Sham one-electron energy;δ_i — density functional approximation (DFA) defect. Other words we obtained empirical corrections δ_i to the calculated orbital energies, which depend on the nature of the orbitals, in such a way that a good correlation is obtained between calculated (corrected) orbital energies and experimental ionization energies.

The bands in the ultraviolet photoelectron spectra corresponding to several orbitals were divided into Gaussians. When dividing spectral bands into Gaussian components, we gave consideration to the number of calculated electron levels, the energy intervals between them and the proximity of ionization cross-section values. The energies of Gaussian maximums IE_g were adopted as IE_i values.

When considering the dependence of the DFA defect on the nature of the electron level, we can compare the experimental IE_i and calculated energies ε_i with an accuracy of 0.1 eV using DFA defect [53–56]. A comparison of experimental and calculated data on IE for 11 boron β-diketonates that we investigated in Refs. [18–20] has shown that δ_i dependence on the nature of MO results in a mean deviation of 0.06 eV for 79 levels.

To evaluate the dependence of δ_i on the nature of the MOs of complexes I–VII, we have compared the vertical IE values published in Ref. [57] with our calculated ε_i values for nitrogen-containing molecules with condensed cycles (indole, benzimidazole) and several six-membered cycles $C_{6-n}H_{6-n}N_n$ (n = 1, 2, 3). For MOs with a dominant contribution by nitrogen n-orbitals, the DFA defect δ_N are 0.1–0.3 eV higher than the DFA defect δ_C of delocalized carbon π-orbitals.

3. Results and discussion

According to our calculated data, molecule I is symmetrical relative to the two fold axis passing across the B and N3 atoms. All atoms of the condensed cycles of complexes II–IV lie in one plane. A deviation from the flat structure of the condensed cycles was found

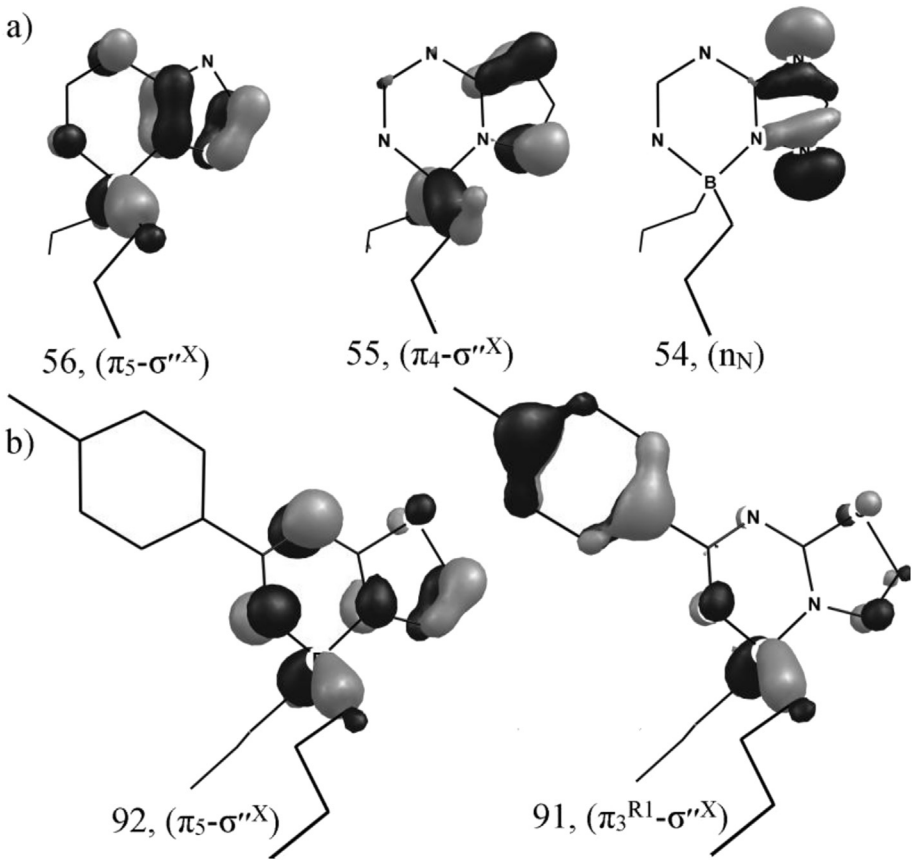

Fig. 4. Some molecular orbitals of compounds II (a) and V (b).

Table 1
Fragments of molecules I–VII.

Complex, fragment	I	II	III	IV	V	VI	VII
X	$(C_3H_7)_2B$			$(C_4H_9)_2B$		$(C_3H_7)_2B$	
β	–N–C–N–C–N-						
Z	–	=N–CH=N–		-S-CH=CH-		–N=CH–CH=CH–	
R_1	C_2H_5	H	$C_6H_4CH_3$	H	$C_6H_4CH_3$	$C_6H_{11}NH$	
R_2	H					C_6H_{11}	

in the row of compounds V–VII. For complex V, the dihedral angle between the planes of the N1–C2–N3–C4–N8 chelate fragment and the N1–B–N8 fragment is equal to 12°. The dihedral angle between the condensed cycle plane and the B–N1–C2 fragment of complexes VI and VII is 12° and 14°. For III and V, the dihedral angle between the planes of chelation and the benzene cycles (substituent is R_1) is 38° and 22°, respectively.

Figs. 1 and 2 show the PE spectra of vapours (thick line) of compounds I–VII and divided Gaussian components (thin circumfluent line). The vertical lines in these spectra correspond to the calculated electron energy values shifted by the values $\overline{\delta}_i$ averaged for each complex (for n_N levels, $\delta_N = \overline{\delta}_i + 0.2$ eV). The dotted lines indicate the nearest calculated electron levels, for which have not been determined IE. The boron diethyl acetylacetonate spectrum [19] is indicated by a dotted line on the spectrum of compound I (Fig. 1).

Orbital forms interesting for the interpretation of PE spectra are shown in Figs. 3 and 4 for complexes I, Ia, II and V. The dominant

Table 2
Electron density localization (%), experimental and calculated energy levels (eV), and effective charges of the fragments (NBO [58]) of compounds I and Ia.

MO number, type	Electron density localization			$-\varepsilon_i$	IE_g	MO number, type	Electron density localization			$-\varepsilon_i$
	2NH	$2C_\beta$	N_γ				2O	$2C_\beta$	$C_\gamma H$	
Compound I						Compound Ia				
π_3-σ''^X	29	3	20	5.76	7.75	σ''^X-π_3	20	3	16	6.16
n_N	8	13	65	7.34	9.41	σ''^X+π_3	12	11	25	7.64
σ''^X+π_3	14	6	20	7.57	9.66	σ'^X	4	1	0	7.89
σ'^X	6	2	9	7.72	9.87	n_-	52	10	6	7.95
Charges	−0.53	1.05	−0.63			Charges	−1.14	1.10	−0.28	

Table 3
Electron density localization (%), experimental and calculated energy levels, and DFA defect (eV) of compounds II–III.

MO Number, type	Electron density localization					$-\varepsilon_i$	IE_g	δ_i
	X	β	Z	R_1	R_2			
Compound II								
56, (π_5-σ''^X)	34	40	26	0	0	6.09	7.99	1.90
55, (π_4-σ''^X)	40	16	44	0	0	7.08	9.24	2.16
54, (n_N)	1	7	92	0	0	7.33	9.53	2.20
Compound III								
80, (π_5-σ''^X)	33	41	26	0	0	5.87	7.66	1.79
79, (π_4-σ''^X)	39	14	41	6	0	6.81	8.65	1.84
78, (n_N)	1	7	92	0	0	7.13	9.14	2.01
77, (π_3+σ''^X)	20	31	39	10	0	7.46	9.30	1.84
76, (σ'^X)	71	11	13	5	0	7.58	9.52	1.94
75, (π_3^{R1}-σ'^X)	23	7	5	65	0	7.80		
74, (π_2^{R1})	0	0	0	100	0	7.97		

Table 4
Electron density localization (%), experimental and calculated energy levels, and DFA defect (eV) of compounds IV–V.

MO number, type	Electron density localization					$-\varepsilon_i$	IE_g	δ_i
	X	β	Z	R_1	R_2			
Compound IV								
68, (π_5-σ''^X)	26	50	24	0	0	5.75	7.70	1.95
67, (σ''^X-π_4^β)	56	8	36	0	0	7.08	9.15	2.07
Compound V								
92, (π_5-σ''^X)	24	50	25	1	0	5.61	7.50	1.89
91, (π_3^{R1}-σ''^X)	26	9	15	50	0	6.63	8.61	1.98
90, (π_2^{R1})	1	1	0	98	0	7.17	9.22	2.05
89, (π_2^{R1}-σ''^X)	31	8	21	40	0	7.19	9.28	2.09

Table 5
Electron density localization (%), experimental and calculated energy levels, and DFA defect (eV) of compounds VI–VII.

MO	Electron density localization					$-\varepsilon_i$	IE_g	δ_i
	X	β	Z	R_1	R_2			
Compound VI								
110, (π_5-σ''^X)	19	49	28	1	3	5.35	6.97	1.62
109, (π_4-π^{R1}-σ''^X)	22	24	15	35	4	6.19	7.88	1.69
108, (σ''^X+π_3)	49	18	14	14	5	6.96	8.80	1.84
Compound VII								
109, (π_5-σ''^X)	25	54	17	0	4	5.56	7.15	1.59
108, (π^{R1}-π_4)	9	27	12	49	3	6.30	7.90	1.60
107, (n_N-σ''^X)	31	27	37	3	2	6.99	8.77	1.78
106, (n_N-σ''^X)	33	16	41	6	4	7.24	9.01	1.77
105, (n_N)	19	66	4	5	6	7.32	9.22	1.90

localization of MOs on molecular fragments is shown by different indices (see Table 1). Tables 2–5 present the relative contributions by MO of the calculated and experimental energies of electron levels for the investigated compounds. The local symmetry C_S relative to the chelate ligand plane is used for BC_2-bonding orbitals (σ^X). The designation n_N is used for σ-type orbitals localized primarily on nitrogen atoms. Based on the calculated data for compounds II–VII, we have plotted a correlation diagram for the top π- and σ-MOs (Fig. 5).

The substitution of the N3 atom and two NH-groups at positions 1 and 5 (complex I) for a CH group and oxygen atoms (compound Ia) results in stabilization of the energy of the four top occupied MOs at 0.2–0.4 eV (Table 2). The high negative charge of oxygen atoms, −1.14, induced primarily by carbonyl atoms of carbon, determines the higher degree of ionic character of the boron bonds for compound Ia. The boron atom charge in complexes I and Ia is 0.63 and 0.88. Therefore, the substitution of O for NH noticeably reduces

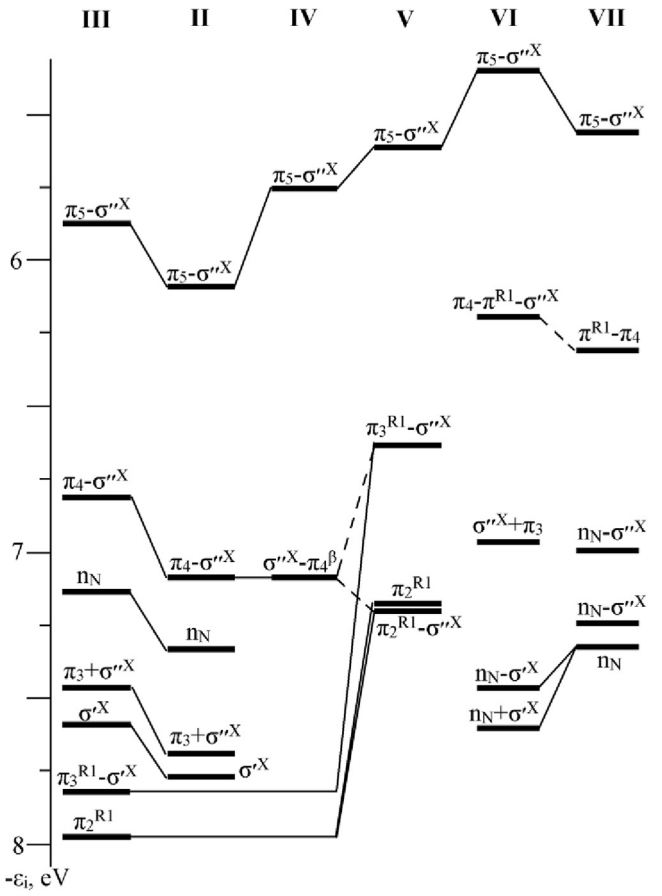

Fig. 5. The correlation diagram of the upper π- and σ-MO of compounds II—VII.

the ionic character of boron bonds and increases covalence. Bond orders are $P_{B-O} = 0.72$ and $P_{B-N} = 0.77$. The second top occupied orbital n_N of complex I is localized primarily on the N3 atom (Table 2, Fig. 3). There is an orbital of n- atoms of oxygen present in compound Ia among the four top occupied MOs (Table 2, Fig. 3). When the interaction of the π-systems of the chelation cycle and complexing agent in complexes I and Ia was analysed, noticeable mixing of π_3^β and σ''^X orbitals was found (Table 2), which is observed for boron acetylacetonates with organic substituents [19].

The first band in the PE spectrum of complex I was induced by ionization from the π_3-σ''^X orbital (Figs. 1 and 3). The second band corresponds to three MOs (Figs. 1 and 3, Table 2). The IE values of boron diethyl acetylacetonate [19] are 0.4–0.7 eV higher than the IE values of complex I (Fig. 1).

There are five π-orbitals, one pseudo-π-MO σ''^X, and one (compounds IV–VI) or two (compounds II–III, VII) MOs n_N present on condensed cycles of complexes II–VII. The n_N orbitals are localized primarily (50–70%) on the N5, N7 atoms (compounds II and III), N3 (complexes IV–VI) and N3, N5 (substance VII). Noticeable mixing of chelate ligand π-orbitals and MO σ''^X was registered for complexes II–VII as well (Tables 3–5, Figs. 3 and 4). The first bands in the PE spectra of compounds II–VII (see Figs. 1 and 2) were induced by ionization from MO π_5-σ''^X.

In accordance with our calculated results, the five top occupied MOs of complexes II–III have similar characters (Fig. 5). In the case of aromatic substituent addition (compound III), the energies of the five top occupied orbitals become destabilized by 0.2–0.3 eV (Fig. 5, Table 3). The second band in the spectra of complexes II and III corresponds to two and one MO, respectively (Fig. 1, Table 3). The

theoretical energy interval of 0.94 eV between the two top occupied MOs of complex III is well consistent with the experimental value $\Delta IE_{1-2} = 0.99$ eV (Table 3, Fig. 1). The third band in the spectrum of compound III is induced by three orbitals (Fig. 1, Table 3). The range of spectra at 10 eV (Fig. 1) corresponds to the $\pi_3 + \sigma''^{X}$ orbital (complex II) or the MO localized primarily on the R_1 substituent (complex III). According to our calculations, the 2′ inflection in the spectrum of compound II (Fig. 1) was induced by the products of thermal destruction of the sample.

The substitution of nitrogen atoms in the five-membered cycle (compound II) for a sulphur atom and CH-group (complex IV) results in destabilization of the energies of the top occupied MO by 0.3 eV (Fig. 5, Tables 3 and 4). The electronic levels of MO π_3^{R1} and π_2^{R1} of compound V are 1.2 and 0.8 eV higher than the respective levels of complex III (Fig. 5, Tables 3 and 4). This result is explained by the acceptor properties of nitrogen atoms of the five-membered cycle (fragment Z charge is −0.47), which took away electronic density from the six-membered cycle.

Unlike boron β-diketonates [18,20], there is no noticeable mixing of the ligand π-orbitals and the benzene cycle MOs for complexes III and V (see Tables 3 and 4, Fig. 4).

The IE_1 values of compounds IV–V are 0.2–0.3 eV smaller than the IE_1 values of compounds II–III (Tables 3 and 4, Fig. 1). The maximum at 9.15 eV in the spectrum of complex IV was induced by processes of ionization from MO σ''^{X}-π_4 (Table 4, Fig. 1). The second and third bands in the PE spectrum of compound V were induced by processes of ionization from three π-orbitals of the R_1 substituent (Fig. 1, Table 4). The area of spectra IV–V at 10 eV (Fig. 1) corresponds to MO n_N-σ''^{X}.

The presence of C_6H_{11} and $C_6H_{11}NH$ substituents in complexes VI and VII results in noticeable delocalization of orbitals (Table 5). The presence of a nitrogen atom in the condensed cycle (compound VII) results in stabilization of the energy of the top occupied MO at 0.2 eV (Fig. 5, Table 5). Noticeable mixing of the chelate ligand orbitals and $C_6H_{11}NH$ group was observed for compounds VI–VII (Table 5).

The IE_1 value of compound VII is 0.2 eV higher than the IE_1 value of complex VI (Table 5, Fig. 2). The second band in complexes VI–VII (Fig. 2) is induced by MO π_4-π^{R1}-σ''^{X} (VI) and the π^{R1}-π_4 orbital (VII). The third band beginning in the spectrum of compound VI (Fig. 2) corresponds to MO $\sigma''^{X} + \pi_3$ and is followed by the n_N-σ''^{X} orbital. The third band in the spectrum of compound VII is induced by three MOs (Fig. 2, Table 5). The spectral area at 9.5 eV (Fig. 2) corresponds to the σ''^{X} orbital.

4. Conclusion

Noticeable mixing of the BC_2 bonding orbitals and π-MOs of the chelation cycle, which is also observed for boron β-diketonates, was recorded for the series of investigated compounds. No noticeable mixing of the orbitals of benzene and chelation cycles, typical of boron β-diketonates, was observed for complexes containing a 4-$C_6H_4CH_3$ substituent. However, mixing of the orbitals of the chelate ligand and $C_6H_{11}NH$ group was observed for compounds VI–VII. The presence of nitrogen atoms in the five-membered cycle (compounds II–III) leads to stabilization of the electron energies of the top occupied MOs at 0.2–0.3 eV and the π_3 and π_2 orbitals of the benzene cycle at 1.2 and 0.8 eV, respectively.

For complexes I, II, III, IV, V, VI and VII, the maximum difference between theoretical and experimental energies with allowance for mean values $\overline{\delta}_i$ (DFA defect δ_N is higher by 0.2 eV) of 2.08; 2.03; 1.85; 2.01; 2.00; 1.72 and 1.60 eV is 0.13 eV, with an average deviation of 0.06 eV.

Acknowledgements

The work was performed with in the State Contract (No. 1137) of the Ministry of Education and Science of the Russian Federation and supported by the Scientific Foundation of the Far Eastern Federal University (grant 12-03-13008-16/13).

References

[1] G. Gorlitz, H. Hartmann, J. Kossanyi, P. Valat, V. Wintgens, Ber. Bunsenges. Phys. Chem. 102 (1998) 1449–1458.
[2] A. Sakai, M. Tanaka, E. Ohta, Y. Yoshimoto, K. Mizuno, H. Ikeda, Tetrahedron Lett. 53 (2012) 4138–4141.
[3] I. Sanchez, J.A. Campo, J.V. Heraset, M. Cano, E. Oliveira, Inorg. Chim. Acta 381 (2012) 124–136.
[4] E.V. Fedorenko, A.G. Mirochnik, A.Yu Beloliptsev, V.V. Isakov, Dyes Pigment. 109 (2014) 181–188.
[5] W.A. Morris, T. Liu, C.L. Fraser, J. Mater. Chem. C 3 (2015) 352–363.
[6] P. Czerney, G. Haucke, C. Igney, Ger. East. DD 265266. 1987. CA 112 (45278) (1990).
[7] M. Halik, G. Schmid, L. Davis, Ger. Pat. 10152938. CA 123 (378622) (2003).
[8] T.E. Goliber, J.H. Perlstein, J. Chem. Phys. 80 (1984) 4162–4167.
[9] S.J. Baker, T. Akama, Y. Zhang, V. Sauro, C. Pandit, R. Singh, M. Kully, J. Khan, J.J. Plattner, S.J. Benkovic, V. Lee, K.R. Maples, Bioorg. Med. Chem. Lett. 16 (2006) 5963–5967.
[10] A. Flores-Parra, R. Contreras, Coord. Chem. Rev. 196 (2000) 85–124.
[11] V.I. Vovna, M.V. Kazachek, I.B. Lvov, Opt. Spectrosc. 112 (2012) 497–505.
[12] S. Xu, R.E. Evans, T. Liu, G. Zhang, J.N. Demas, C.O. Trindle, C.L. Fraser, Inorg. Chem. 52 (2013) 3597–3610.
[13] S. Chibani, A. Charaf-Eddin, B. Mennucci, B. Le Guennic, D. Jacquemin, J. Chem. Theory Comput. 10 (2014) 805–815.
[14] G. Bai, C. Yu, C. Cheng, E. Hao, Y. Wei, X. Mu, L. Jiao, Org. Biomol. Chem. 12 (2014) 1618–1626.
[15] M.V. Kazachek, I.V. Svistunova, Spectrochim. Acta Part A Mol. Biomol. Spectrosc. 148 (2015) 60–65.
[16] O.L. Shcheka, A.V. Borisenko, V.I. Vovna, Russ. J. Gen. Chem. 62 (1992) 489–494.
[17] V.F. Traven, A.V. Manaev, T.A. Chibisova, J. Electron Spectrosc. Relat. Phenom. 149 (2005) 6–10.
[18] V.I. Vovna, S.A. Tikhonov, M.V. Kazachek, I.B. Lvov, V.V. Korochentsev, E.V. Fedorenko, A.G. Mirochnik, J. Electron Spectrosc. Relat. Phenom. 189 (2013) 116–121.
[19] S.A. Tikhonov, I.B. Lvov, V.I. Vovna, Rus. J. Phys. Chem. B 8 (2014) 626–633.
[20] V.I. Vovna, S.A. Tikhonov, I.B. Lvov, I.S. Osmushko, I.V. Svistunova, O.L. Shcheka, J. Electron Spectrosc. Relat. Phenom. 197 (2014) 43–49.
[21] Q.-D. Liu, M.S. Mudadu, R. Thummel, Y. Tao, S. Wang, Adv. Funct. Mater. 15 (2005) 143–154.
[22] G. Naixun, C. Chi, Yu Changjiang, H. Erhong, W. Shengyuan, W. Jun, W. Yun, M. Xiaolong, J. Lijuan, Dalton Trans. 43 (2014) 7121–7127.
[23] Y. Deng, Y. Cheng, H. Liu, J. Mack, H. Lu, L. Zhu, Tetrahedron Lett. 55 (2014) 3792–3796.
[24] E.K.U. Gross, E. Runge, O. Heinonen, Many Particle Theory, Adam Hilger, 1992.
[25] E.N. Economou, Green's Functions in Quantum Physics, Springer, New York, 1979.
[26] S. Hamel, P. Duffy, M.E. Casida, D.R. Salahub, J. Electron. Spectr. Relat. Phenom. 123 (2002) 345–363.
[27] P. Duffy, D.P. Chong, M.E. Casida, D.R. Salagub, Phys. Rev. A 50 (1994) 4707–4728.
[28] D.P. Chong, O.V. Gritsenko, E.J. Baerends, J. Chem. Phys. 116 (2002) 1760–1772.
[29] O.V. Gritsenko, E.J. Baerends, J. Chem. Phys. 117 (2002) 9154–9162.
[30] O.V. Gritsenko, B. Braïda, E.J. Baerends, J. Chem. Phys. 119 (2003) 1937.
[31] B.S. Jursic, J. Mol. Struc. Theochem. 452 (1998) 145.
[32] U. Mölder, R. Pikver, I.I. Koppel, P. Burk, I.A. Koppel, J. Mol. Struct. Theochem. 579 (2002) 205.
[33] J. Jellinek, P.H. Acioli, J. Chem. Phys. 118 (2003) 7783.
[34] B.M. Mikhailov, V.A. Dorokhov, V.I. Seredenko, Bull. Acad. Sci. USSR Div. Chem. Sci. 27 (1978) 1205–1210.
[35] V.A. Dorokhov, L.I. Lavrinovich, B.M. Mikhailov, Bull. Acad. Sci. USSR Div. Chem. Sci. 29 (1980) 481–485.
[36] V.A. Dorokhov, B.M. Zolotarev, B.M. Mikhailov, Bull. Acad. Sci. USSR Div. Chem. Sci. 30 (1981) 649–653.
[37] V.A. Dorokhov, A.R. Amamchyan, M.N. Bochkareva, I.A. Teslya, Z.A. Starikova, Bull. Acad. Sci. USSR Div. Chem. Sci. 36 (1987) 147–151.
[38] A.A. Granovsky, Firefly version 7.1.G, http://classic.chem.msu.su/gran/firefly/index.html.
[39] Basis Set Exchange. Version 1.2.2: https://bse.pnl.gov/bse/portal.
[40] M. Marsman, J. Paier, A. Stroppa, G. Kresse, J. Phys. Condens. Matter 20 (2008) 064201.
[41] L. Goerigk, S. Grimme, Wiley Interdiscip. Rev. Comput. Mol. Sci. 6 (2014) 576–600.
[42] Y. Zhao, D.G. Truhlar, Chem. Phys. Lett. 502 (2011) 1–13.

[43] A.E. Raeber, B.M. Wong, J. Chem. Theory Comput. 11 (2015) 2199–2209.
[44] A. Prlj, B.F.E. Curchod, A. Fabrizio, L. Floryan, C. Corminboeu, J. Phys. Chem. Lett. 6 (2015) 13–21.
[45] S. Grimme, J. Antony, S. Ehrlich, H. Krieg, J. Chem. Phys. 132 (2010) 154104–154118.
[46] S. Ogawa, M. Morikawa, G. Juhasz, N. Kimizuka, RSC Adv. 5 (2015) 60373–60379.
[47] Y. Kubota, K. Kasatani, H. Takai, K. Funabiki, M. Matsui, Dalton Trans. 44 (2015) 3326–3341.
[48] M.-C. Chang, E. Otten, Inorg. Chem. 54 (2015) 8656–8664.
[49] I.S. Osmushko, V.I. Vovna, S.A. Tikhonov, Y.V. Chizhov, I.V. Krauklis, Int. J. Quantum Chem. 116 (2016) 325–332.
[50] A.D. Becke, J. Chern. Phys. 98 (1993) 5648–5652.
[51] C. Lee, W. Yang, R.G. Parr, Phys. Rev. B 37 (1988) 785–789.
[52] P.J. Stevens, F.J. Devlin, C.F. Chablowski, M.J. Frisch, J. Phys. Chem. 98 (1994) 11623–11627.
[53] I.V. Krauklis, Yu.V. Chizhov, Opt. Spectrosc. 96 (2004) 47–54.
[54] I.V. Krauklis, Yu.V. Chizhov, Opt. Spectrosc. 98 (2005) 341–348.
[55] V.I. Vovna, V.V. Korochentsev, A.A. Komissarov, I.B. L'Vov, N.S. Myshakina, J. Mol. Struct. 1099 (2015) 579–587.
[56] V.I. Vovna, S.A. Tikhonov, I.B. Lvov, Russ. J. Phys. Chem. A 87 (2013) 688–693.
[57] V.I. Vovna, Electronic Structure of Organic Compounds: Photoelectron Data, Nauka, Moscow, 1991 (in Russian).
[58] A.E. Reed, L.A. Curtiss, F. Weinhold, Chem. Rev. 88 (1988) 899–926.